Supplemental material

Razzell et al., https://doi.org/10.1083/jcb.201801171

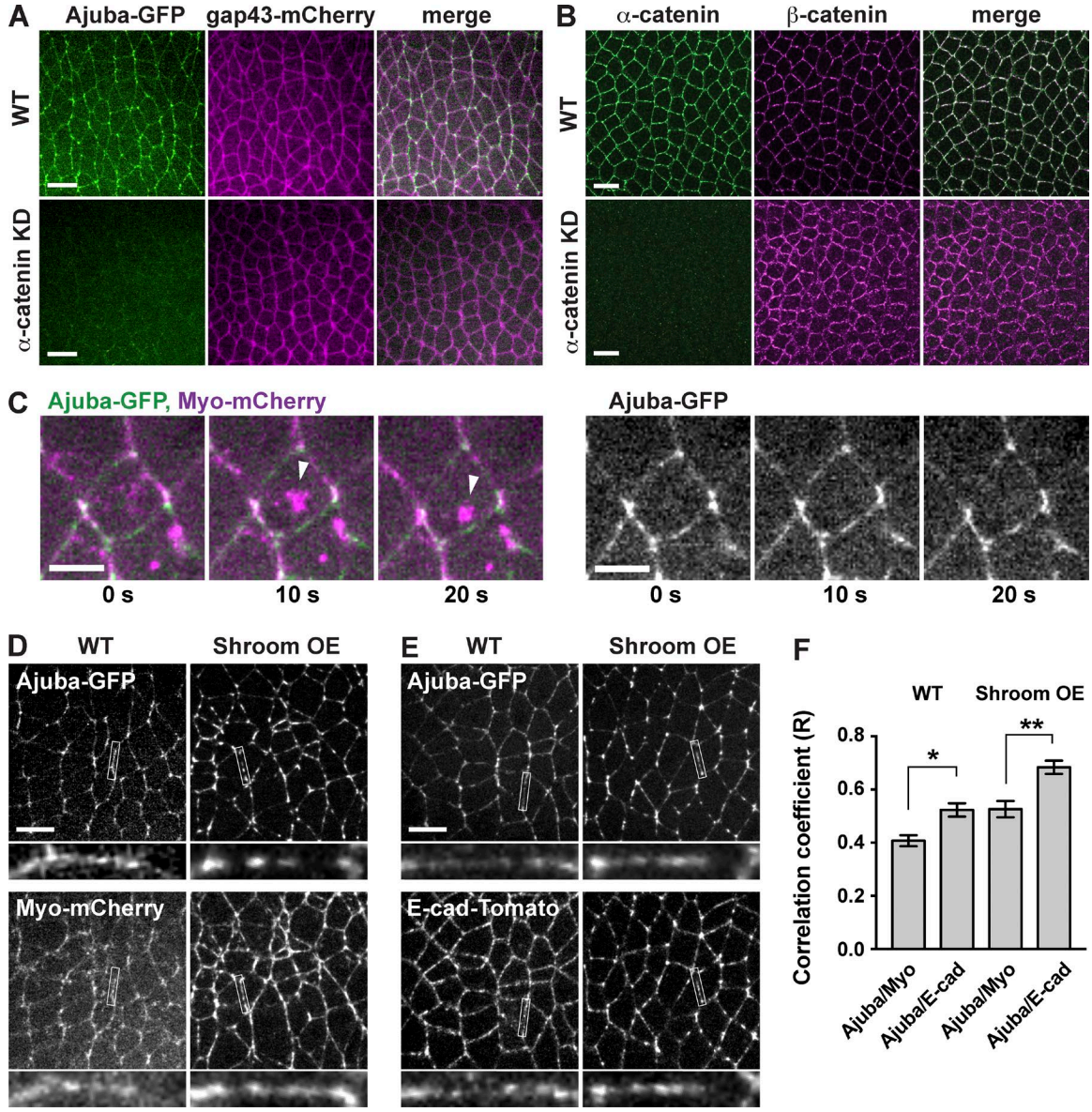

Figure S1. **Ajuba localizes to adherens junctions in WT and ShroomA-overexpressing embryos.** Related to Figs. 1 and 2. **(A)** Living WT and α-catenin shRNA–expressing (α-catenin KD) embryos at stage 7 showing Ajuba-GFP (green) and the membrane marker gap43-mCherry (magenta). Ajuba junctional localization is strongly reduced in α-catenin KD embryos. **(B)** Fixed WT and α-catenin KD embryos at stage 7 immunostained for α-catenin and β-catenin. There is a strong reduction in junctional α-catenin in α-catenin KD embryos, although cortical β-catenin is still present. **(C)** Ajuba-GFP (green) and Myo-mCherry (magenta) imaged in living WT embryos at stage 7. Ajuba does not localize to pulses of myosin accumulation (arrowheads) at the medial cell cortex. **(D)** Ajuba-GFP and Myo-mCherry in WT and ShroomA-overexpressing (Shroom OE) embryos at stage 7. **(E)** Ajuba-GFP and E-cadherin-mTomato in WT and Shroom OE embryos at stage 7. White boxes in D and E correspond to the enlarged regions below each image. **(F)** Correlation coefficients for Ajuba-GFP with Myo-mCherry or E-cadherin-mTomato in WT and Shroom OE embryos. Ajuba-GFP shows a lower correlation with Myo-mCherry in these experiments than in Fig. 1 D because only near-vertical edges are analyzed here, compared with all edges in Fig. 1 D, and protein localization is analyzed by pixel, rather than by edge as in Fig. 1 D. Along vertical edges, the pattern of Ajuba-GFP correlates better with E-cadherin-mTomato than with Myo-mCherry. R values were calculated from scatter plots of myosin versus Ajuba and E-cadherin versus Ajuba pixel intensities. The mean ± SEM between embryos is shown (n = 5 embryos/genotype, 50 interfaces analyzed/embryo); *, P < 0.01; **, P < 0.001; one-way ANOVA with Fisher's least significant difference test. Images are anterior left, ventral down. Bars: (A, B, D, and E) 10 µm; (C) 5 µm.

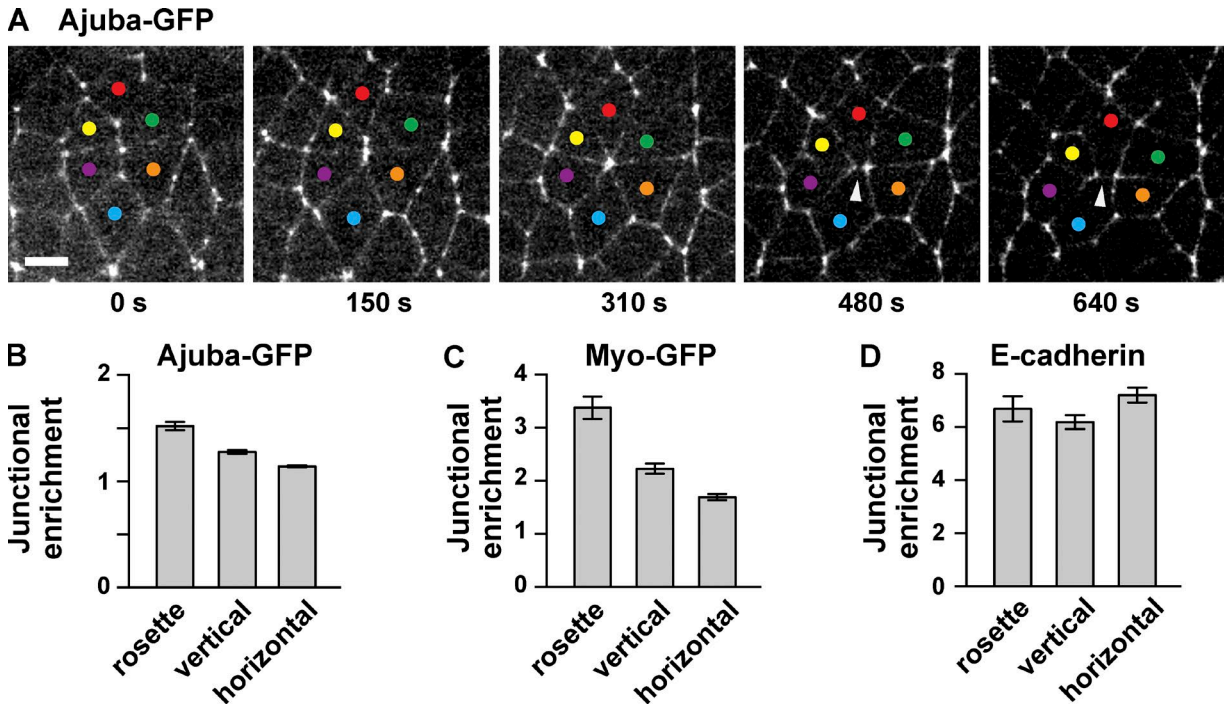

Figure S2. **Ajuba localization during rosette formation.** Related to Fig. 1. **(A)** Stills from a time-lapse video showing Ajuba-GFP localization during rosette formation and resolution. Ajuba-GFP was enriched at shrinking edges and rosette vertices, but was absent from newly formed edges during rosette resolution (arrowhead). **(B)** Localization of Ajuba-GFP to adherens junctions at linked vertical edges in forming rosettes, single vertical edges, and horizontal edges. **(C and D)** Localization of Myo-GFP (C) and E-cadherin (D) in immunostained embryos. Edge intensities were divided by the cytoplasmic intensity to calculate junctional enrichment. The mean ± SEM between interfaces is shown; *n* = 32–44 interfaces/category from videos of seven embryos for Ajuba-GFP and 20–45 interfaces/category from six fixed embryos for Myo-GFP and E-cadherin. Images are anterior left, ventral down. Bar, 5 µm.

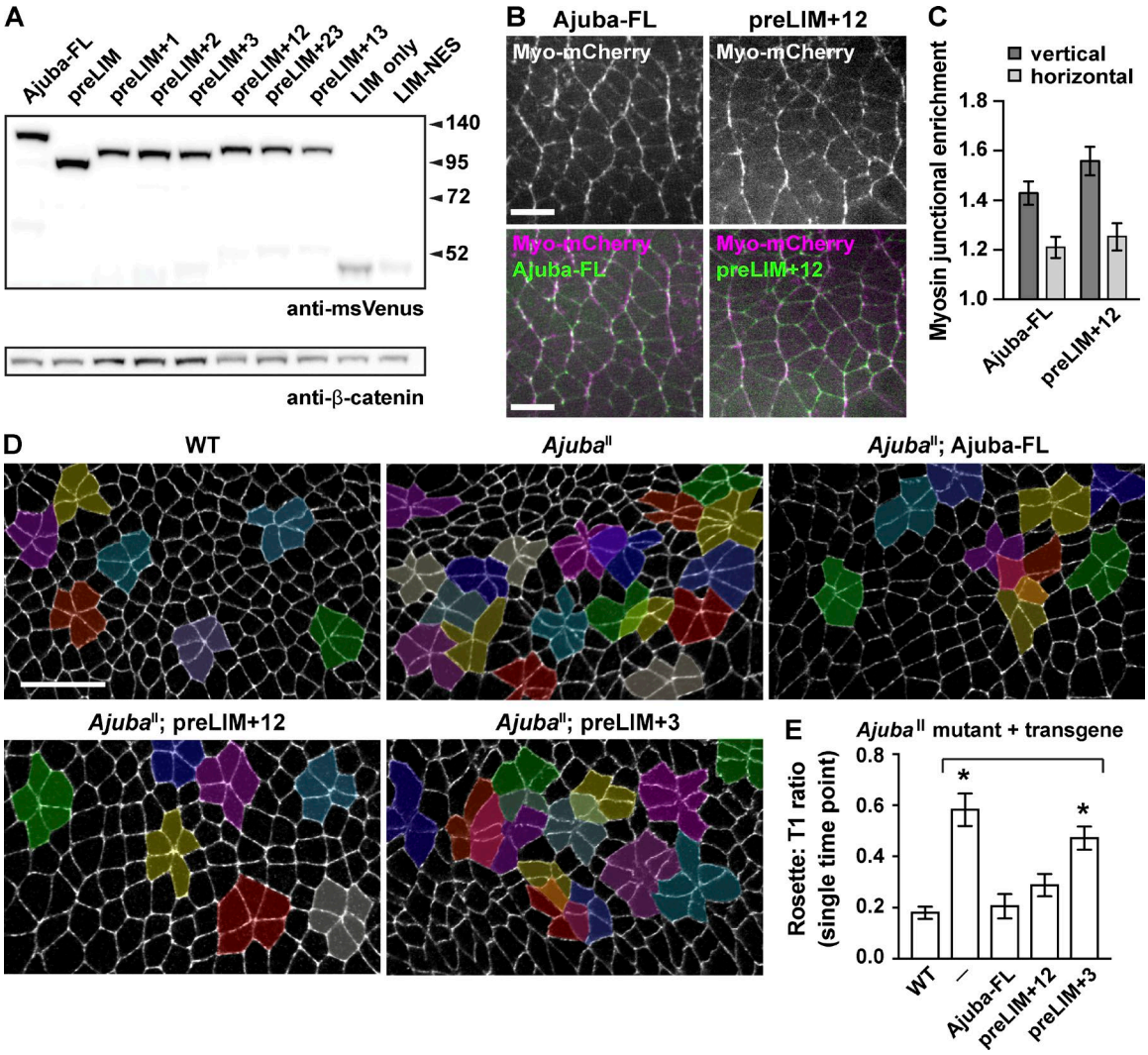

Figure S3. **Characterization of *Ajuba* transgenes.** Related to Figs. 3 and 4. **(A)** Immunoblot of embryo lysates (40 stage 6–8 embryos/lane) showing expression levels of Ajuba-msVenus variants and β-catenin (loading control). A representative example of three independent experiments is shown. **(B)** Myo-mCherry (magenta in merge) and Ajuba-FL-msVenus or preLIM+12-msVenus (green in merge) localization in stage 7/8 embryos. **(C)** Myosin junctional enrichment in embryos expressing Ajuba-FL-msVenus or preLIM+12-msVenus at vertical edges (oriented at 75–90° relative to the AP axis) and horizontal edges (oriented at 0–15° relative to the AP axis). Mean ± SEM between embryos is shown; n = 6 embryos/genotype; 162–353 interfaces analyzed/embryo. **(D)** Fixed stage 8 WT, *Ajuba*^{II} mutant, and *Ajuba*^{II} mutant embryos expressing Ajuba-full length (Ajuba-FL), preLIM+12, or preLIM+3 msVenus-tagged variants and immunostained for E-cadherin. Rosettes with five or more cells are highlighted. **(E)** Rosette:T1 ratio calculated at a single time point in immunostained embryos. Clusters of four cells were identified as T1 processes, and clusters of five or more cells were identified as rosettes if groups of cells shared a common vertex or circumscribed strings of edges that were each less than 1.2 µm in length. The mean ± SEM between embryos is shown (n = 6–7 embryos/genotype); *, P < 0.0001; one-way ANOVA with Fisher's least significant difference test. Images are anterior left, ventral down. Bars: (B) 10 µm; (D) 20 µm.

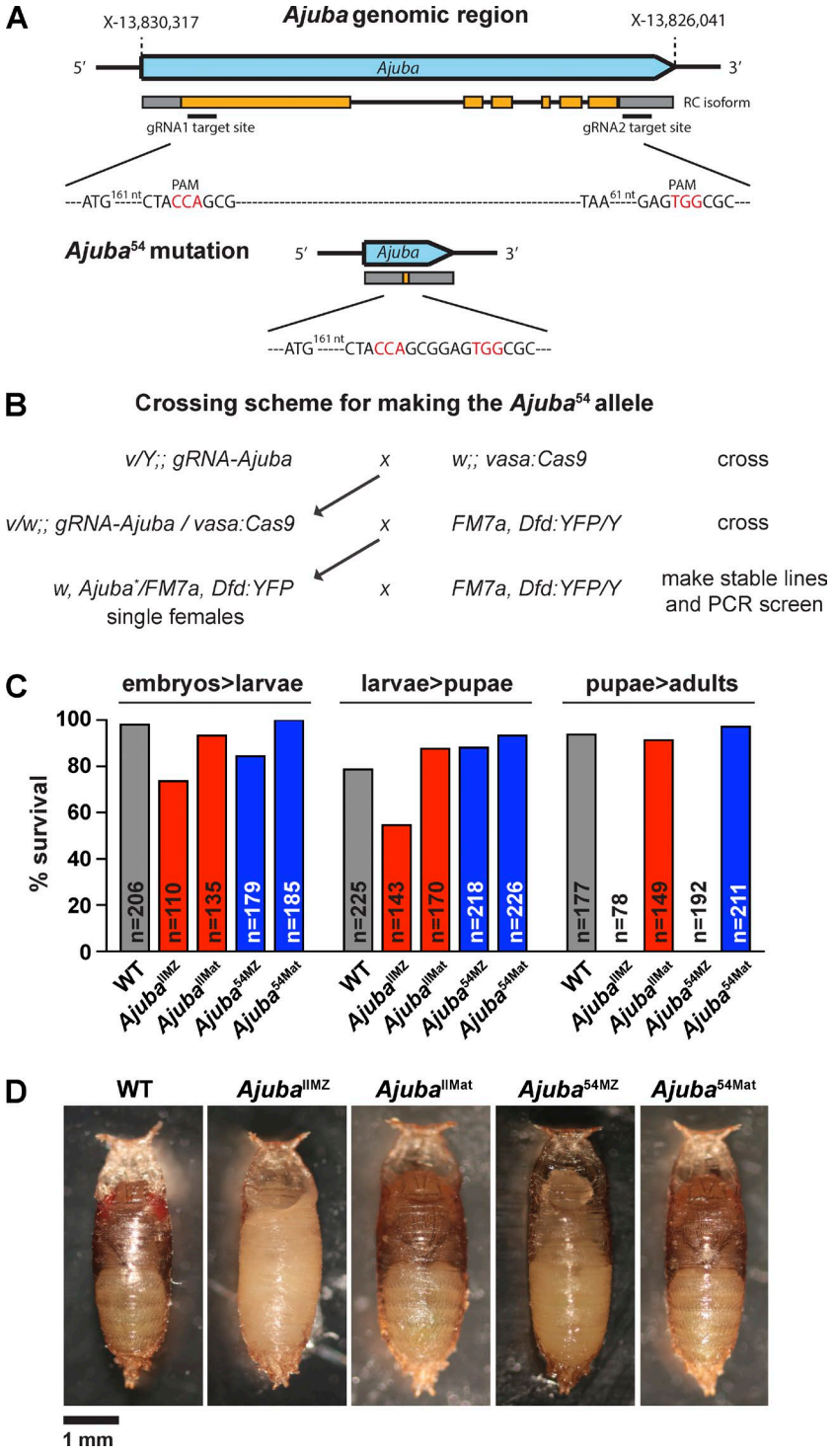

Figure S4. **Generation of an *Ajuba* null allele using CRISPR-mediated mutagenesis.** Related to Figs. 5, 6, 7, and 8. **(A)** The *Ajuba* locus before and after CRISPR mutagenesis and sequence of the *Ajuba*^{54} mutation. The gRNA target sites and PAM recognition motifs are highlighted. **(B)** Crossing scheme used to generate the *Ajuba*^{54} allele using a transgenically expressed gRNA targeting the *Ajuba* locus. **(C)** Percentage survival of WT, *Ajuba* maternally and zygotically mutant embryos (*Ajuba*^{MZ}), and *Ajuba* maternal mutants that have WT zygotic *Ajuba* expression (*Ajuba*^{Mat}) at each stage of *Drosophila* development. **(D)** Images of pupae 120 h after pupal formation (anterior up).

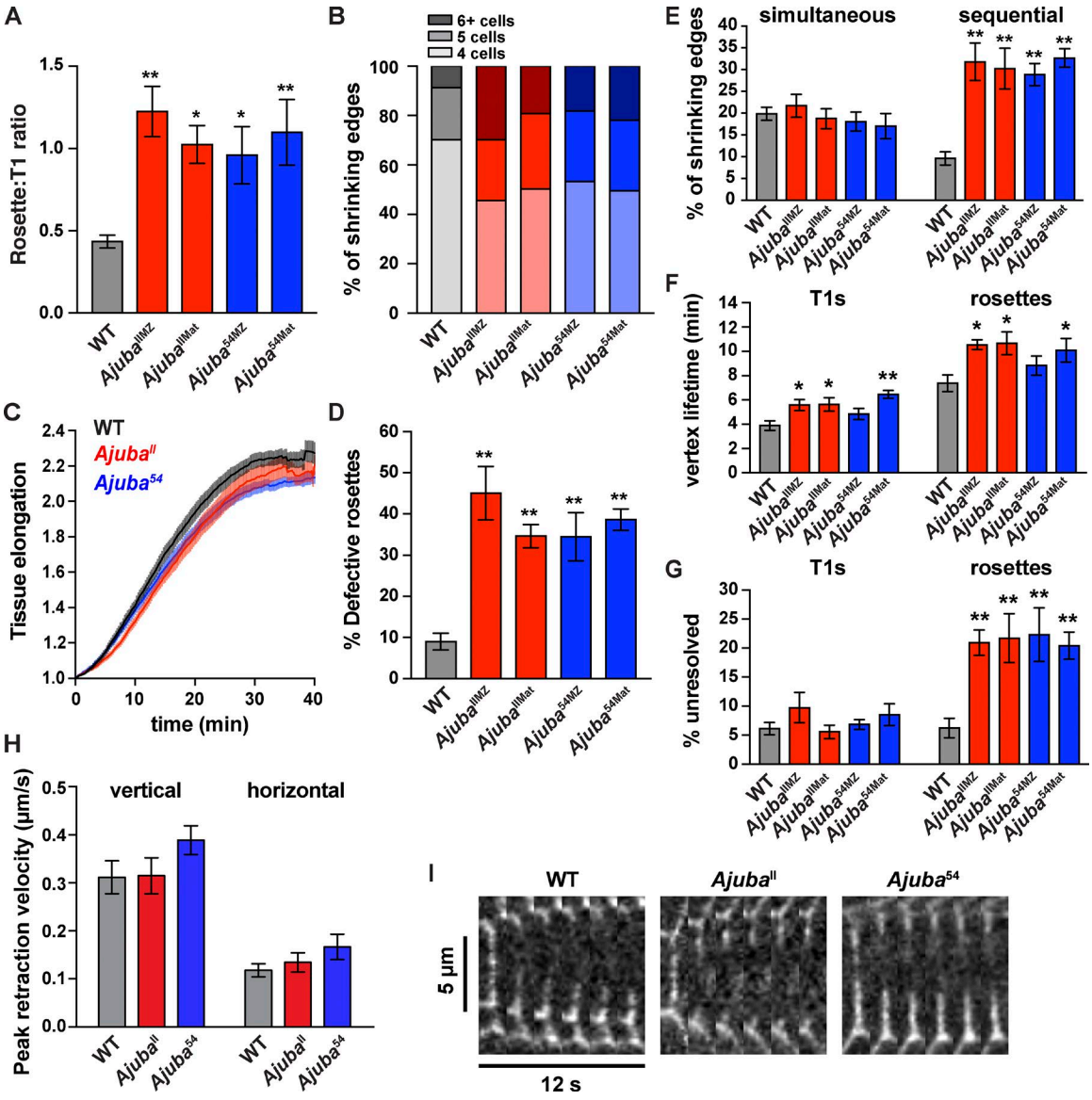

Figure S5. **Cell behaviors in *Ajuba* mutants separated by genotype.** Related to Figs. 5 and 6. **(A)** Rosette:T1 ratio, calculated as the ratio of the number of shrinking edges that joined rosettes or T1 processes during axis elongation in WT, *Ajuba* maternally and zygotically mutant embryos (*Ajuba*^{MZ}), and *Ajuba* maternal mutants that have WT zygotic *Ajuba* expression (*Ajuba*^{Mat}). **(B)** Percentage of shrinking edges that formed four-cell vertices (T1 processes, light shading), five-cell rosettes (medium shading), or rosettes with six or more cells (dark shading). **(C)** Elongation of the anterior and central germband along the AP axis normalized to the length at $t = 0$ (the onset of elongation in early stage 7). **(D)** Percentage of rosettes that displayed gaps between cells. **(E)** Percentage of shrinking edges that formed rosettes through simultaneous or sequential contraction. **(F)** Lifetime of high-order vertices in T1 processes (T1s) or rosettes. **(G)** Percentage of shrinking edges that formed vertices that did not resolve. The mean ± SEM between embryos is shown (n = 6–12 embryos/genotype, 33–49 shrinking edges analyzed/embryo in A, B, E, F, and G; 7–21 rosettes analyzed/embryo in D). **(H)** Peak retraction velocity of ablated vertical and horizontal cell interfaces in WT and *Ajuba* mutant embryos (n = 10 vertical edges and 10 horizontal edges ablated/genotype). **(I)** Kymographs of ablated interfaces in embryos expressing β-catenin-GFP. *, P < 0.05; **, P < 0.001; one-way ANOVA with Fisher's least significant difference test. These embryos were combined for analysis in Figs. 5 and 6.

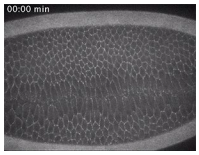

Video 1. **Time-lapse video of convergent extension in a WT embryo expressing β-catenin-GFP.** Images were acquired at 15-s intervals. Anterior left, ventral down.

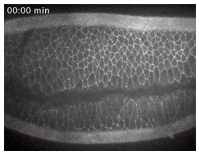

Video 2. **Time-lapse video of convergent extension in an *Ajuba*^{ll} maternally and zygotically mutant embryo expressing β-catenin-GFP.** Images were acquired at 15-s intervals. Anterior left, ventral down.

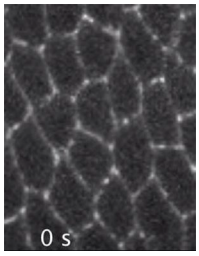

Video 3. **Time-lapse video of a WT embryo expressing β-catenin-GFP showing a normal rosette with junctions tightly apposed.** Images were acquired at 15-s intervals. Anterior left, ventral down.

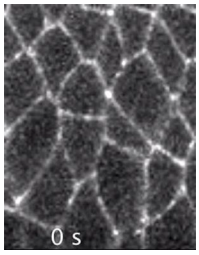

Video 4. **Time-lapse video of an *Ajuba*^{ll} maternally and zygotically mutant embryo expressing β-catenin-GFP showing a rosette with a gap between cells at the rosette vertex.** Images were acquired at 15-s intervals. Anterior left, ventral down.

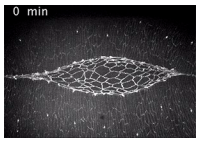

Video 5. **Time-lapse video of dorsal closure in a WT embryo expressing β-catenin-GFP.** Images were acquired at 1-min intervals. Anterior left.

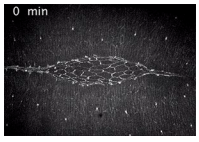

Video 6. **Time-lapse video of dorsal closure in a *shg*^{2}/+ embryo expressing β-catenin-GFP.** Images were acquired at 1-min intervals. Anterior left.

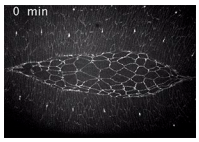

Video 7. **Time-lapse video of dorsal closure in an *Ajuba*^{54} maternally and zygotically mutant embryo expressing β-catenin-GFP.** Images were acquired at 1-min intervals. Anterior left.

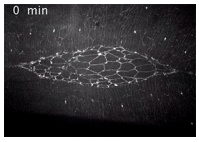

Video 8. **Time-lapse video of dorsal closure in an *Ajuba*^{ll} maternally and zygotically mutant embryo expressing β-catenin-GFP.** Images were acquired at 1-min intervals. Anterior left.

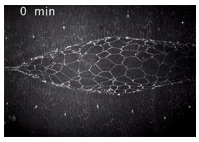

Video 9. **Time-lapse video of dorsal closure in an *Ajuba*^{54} maternally and zygotically mutant embryo that is also heterozygous for *shg*^{2}.** Images were acquired at 1-min intervals. Anterior left.

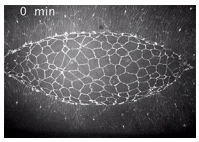

Video 10. **Time-lapse video of dorsal closure in an *Ajuba*^{ll} maternally and zygotically mutant embryo that is also heterozygous for *shg*^{2}.** Images were acquired at 1-min intervals. Anterior left.